SPECTRAL IMAGING OF OSTRACA

Gregory Bearman & William A. Christens-Barry*#

*ANE Image, Pasadena, CA 91104, equipoise1@verizon.net
#Chief Scientist, Equipoise Imaging, LLC, 4009 St. Johns Lane, Ellicott City, MD 21042

Bearman, G. & W.A. Christens-Barry. 2009. Spectral Imaging of Ostraca. – Palarch's Journal of Archaeology of Egypt/Egyptology 6(7) (2009), 1-20. ISSN 1567-214X. 20 pages + 22 figures.

Keywords: ostraca, spectral imaging, archeological imaging

ABSTRACT

By analogy with ancient texts, infrared imaging of ostraca has long been employed to help improve readings. We report on extensive spectral imaging of ostraca over the visible and near infrared. Spectral imaging acquires the complete spectrum for each pixel in an image; the data can be used with an extensive set of software tools that were developed originally for satellite and scientific imaging. In this case, the spectral data helps explain why infrared imaging works to improve text legibility (and why not in some cases). A better understanding of the underlying imaging mechanism points the way for inexpensive methods for taking data either in the field or at museums.

Introduction

Modern imaging technologies have had a significant impact on archeology, from site selection to 3D imaging of a site, documenting finds and strata and finally examination of excavated objects. Texts of all sorts are a natural object for imaging of any sort, since the main goal is always improving readings. In this paper, we report on the application of spectral imaging methods to ostraca, primarily, with some recent new data from the Dead Sea Scrolls and papyri that served as guides for this work.

In the summer of 2008, one of the authors (Bearman, already in Jerusalem working on an imaging project for the Israel Antiquities Authority [IAA]) was invited by Prof. Yosef Garfinkel to examine the recently found ostracon from Khirbet Qeiyafa (http://qeiyafa.huji.ac.il/) less than one month after its discovery. The written text was not well preserved, a condition that imposed great difficulties on its decipherment. Hoping that sophisticated imaging techniques would improve legibility of the text, the excavators took advantage of the coincidence and asked Bearman for a few images. He took some spectral image cubes between 650–1000 nm and provided Misgav Haggai (epigrapher responsible for the ostracon text) with analyzed and processed images; these were sufficient to encourage transport of the ostracon to the US for further imaging studies. We report the various technologies, which provided improved readings for the text scholar and also illuminated the whys of infrared imaging of ostraca in general.

Some of the initial work on imaging the Khirbet Qeiyafa ostracon was based on what is known about color, infrared and spectral imaging from work with other ancient texts. Infrared photography with film, digital infrared imaging and spectral imaging have all been applied to ancient texts. The Dead Sea Scrolls, having been the most extensively studied with all three was used as the model for analysis of the Khirbet Qeiyafa ostracon.

Soon after their invention, both ultraviolet (UV) and infrared (IR) film photography were investigated as tools for imaging texts, documents and archeological artifacts (Beardsley, 1936; Ross, 1933). One of the best known examples in the archeological world is the application of IR photography to papyri and the Dead Sea Scrolls (Plenderleith, 1950). It has long been known that IR film photography dramatically improved text legibility of documents, although the process was poorly understood, and the reasons for its success or failure were not known. Most of the Dead Sea Scroll images used by scholars for the last 60 years have been large-format IR images taken with film and a long pass Kodak filter (Bearman *et al.*, 1998). The explanation came with spectral imaging in the early 1990s (Bearman *et al.*, 1993; Bearman & Spiro, 1996), at least phenomenologically, thus pointing to ways in which digital imaging and bandpass filtering could be used to improve IR imaging.

Beginning in the early 1990s, advances in cameras, software and electo-optical components made it much easier to apply modern digital and spectroscopic methods to ancient objects and art for studies in conservation, preservation and legibility, leading to a significant body of work on the applications of point spectroscopy and spectral imaging to art (Baronti *et al.*, 1997; Mansfield *et al.*, 1999; Attas *et al.*, 2003; Edwards & Perez, 2004; Delaney *et al.*, 2005), conservation, and text legibility (Havermans *et al.*, 2003a, 2003b; Goltz *et al.*, 2007).

Raman spectroscopy (Edwards *et al.*, 1999; Mannucci *et al.*, 2000; Marengo *et al.*, 2003) and IR spectroscopy (Ferrer & Sistach, 2005; Lee *at al.*, 2006) have been used to examine the chemical composition of pigments, substrates and artifacts as well as to track changes in the writing substrate. We did not apply Raman and IR techniques to the ostracon for two reasons: (1) they report primarily on chemistry and geology, which we do not need and (2) spectral imaging with these methods is quite difficult, and even more so for the curved ostracon. There is a clear distinction between point and imaging spectroscopy in these applications. Point spectroscopy is useful for building spectral libraries of pigment and other materials for conservation.

Spectral Imaging of the Dead Sea Scrolls

We want to spend some time arguing the case for using some new results from spectral imaging of the Dead Seas Scrolls and papyrus; both sets of data guided the thinking and setup of the imaging for the ostraca. In the case of the Dead Sea Scrolls and of many papyri, spectral imaging showed that the reduction in visible contrast was due to changes in the reflectance of the ink relative to the parchment (or papyrus) substrate. This is shown in figures 1-4 and figures 5-6 for two different ancient texts – one on animal skin and one on papyrus.

For the legible Dead Sea Scrolls fragments in figure 3, shown at two different wavelengths, the ink and parchment have different enough reflectance in the visible to make the text quite legible in the visible. On the other hand, in figure 4, the fragment is illegible in the visible and legible in the IR; figure 3 shows that the reflectance of the ink and parchment are much closer than they are for the other fragment. Figures 5 and 6 demonstrate the same sort of behavior for a papyrus from the Neptunis Collection at the University of California, Berkeley. In this case, figure 6 shows that the ink and papyrus reflectance are nearly identical throughout most of the visible and there is no real contrast until just at the edge of the sensitivity of the red channel of a CCD color camera. To further illustrate this point, figures 7A and B show images of the same papyrus at 650 nm and 750 nm. Both of these have been adjusted; the dark and white were set to the ink and parchment levels respectively, thus clipping off the data

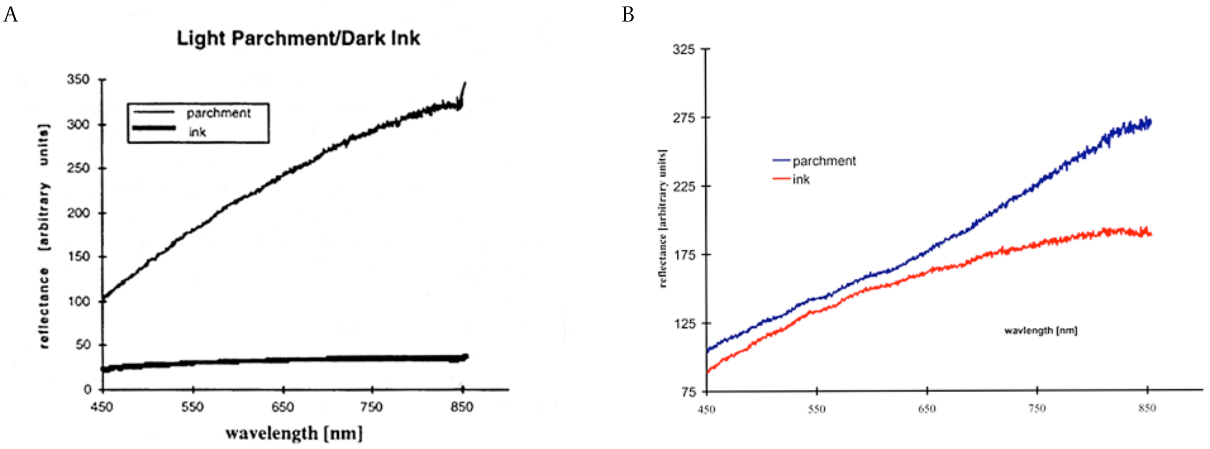

Figure 1. Reflectance spectra of two Dead Sea Scrolls in the visible and near infrared. In A) the image of the text for that fragment is quite legible to the human eye, while for B) it is not. This data was taken with an Ocean Optics point spectrometer and goes out only to 850 nm. For the legible text, the ink and parchment have very different reflectance, while the spectra for the illegible fragment are very similar in the visible.

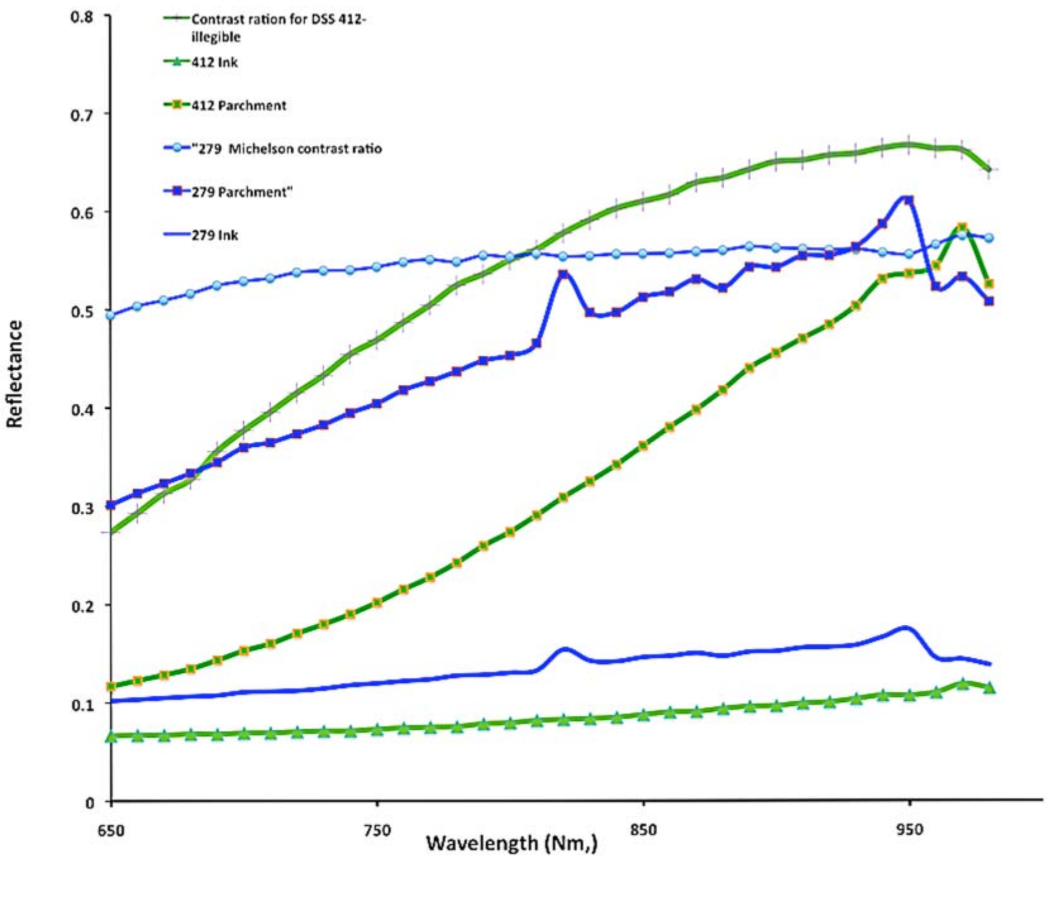

Figure 2. Reflectance spectra of two Dead Sea Scroll fragments acquired during the 2008 Dead Sea Scroll Pilot Imaging Project (Tanner & Bearman, 2009). This data was taken with a spectral imager that covered the range 650 - 1100 nm. The spectra have all been normalized to the illumination source spectra and are true calibrated reflectances.

Figure 3 (p. 4). Two images of IAA inventory plate 279 taken at the extreme ends of wavelengths available during the 2008 Pilot Imaging Project. This fragment is very legible to the human eye and in color and black/white photographs; see figure 2 for the spectra.

A

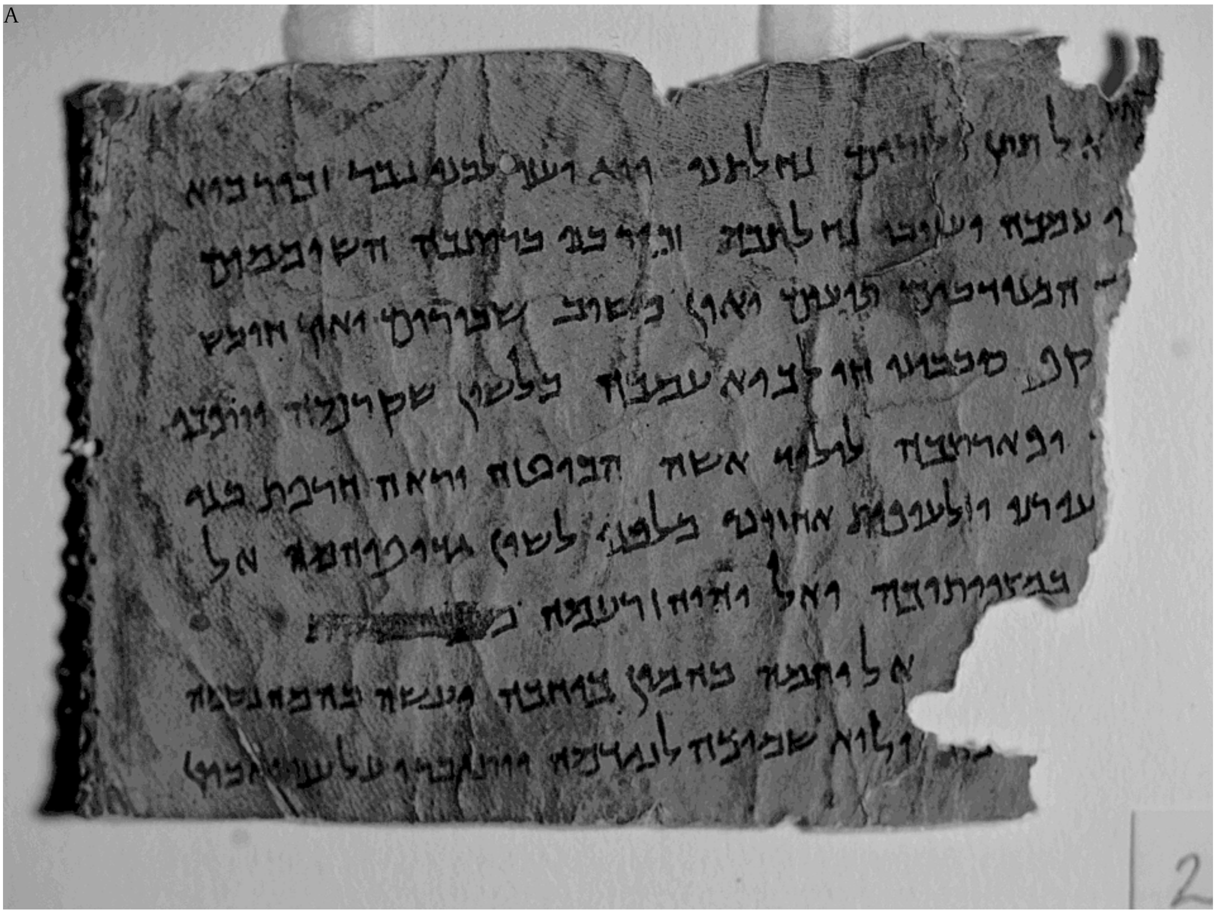

B

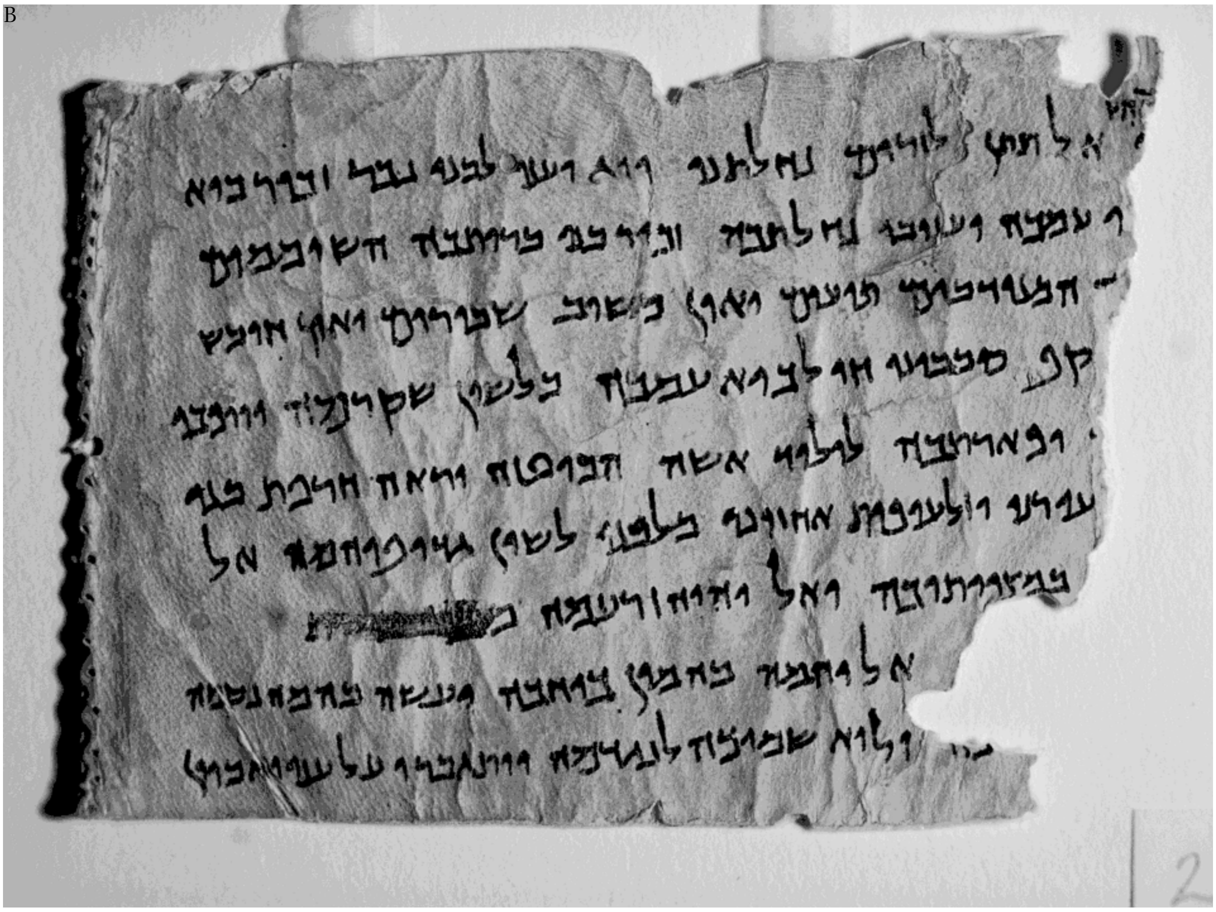

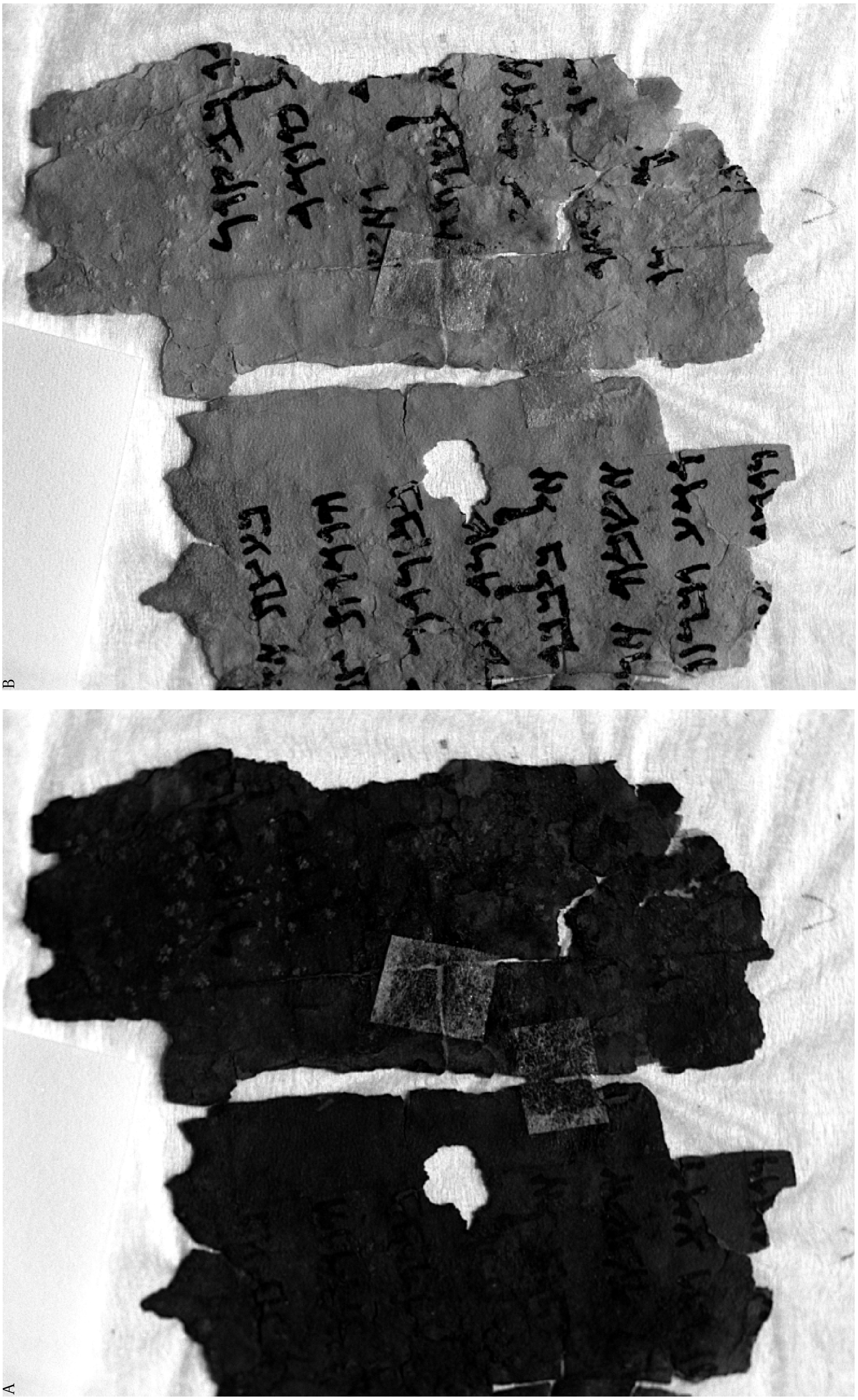

Figure 4. IAA inventory plate 412 imaged at two wavelengths. The spectra can be seen in figure 2. Note that the IR reads through the scotch tape visible on the right side of the fragment. In this case, one can easily see a ש that is obscured at the shorter wavelength. Since the tape has a thin plastic substrate, IR can read through it at longer wavelengths.

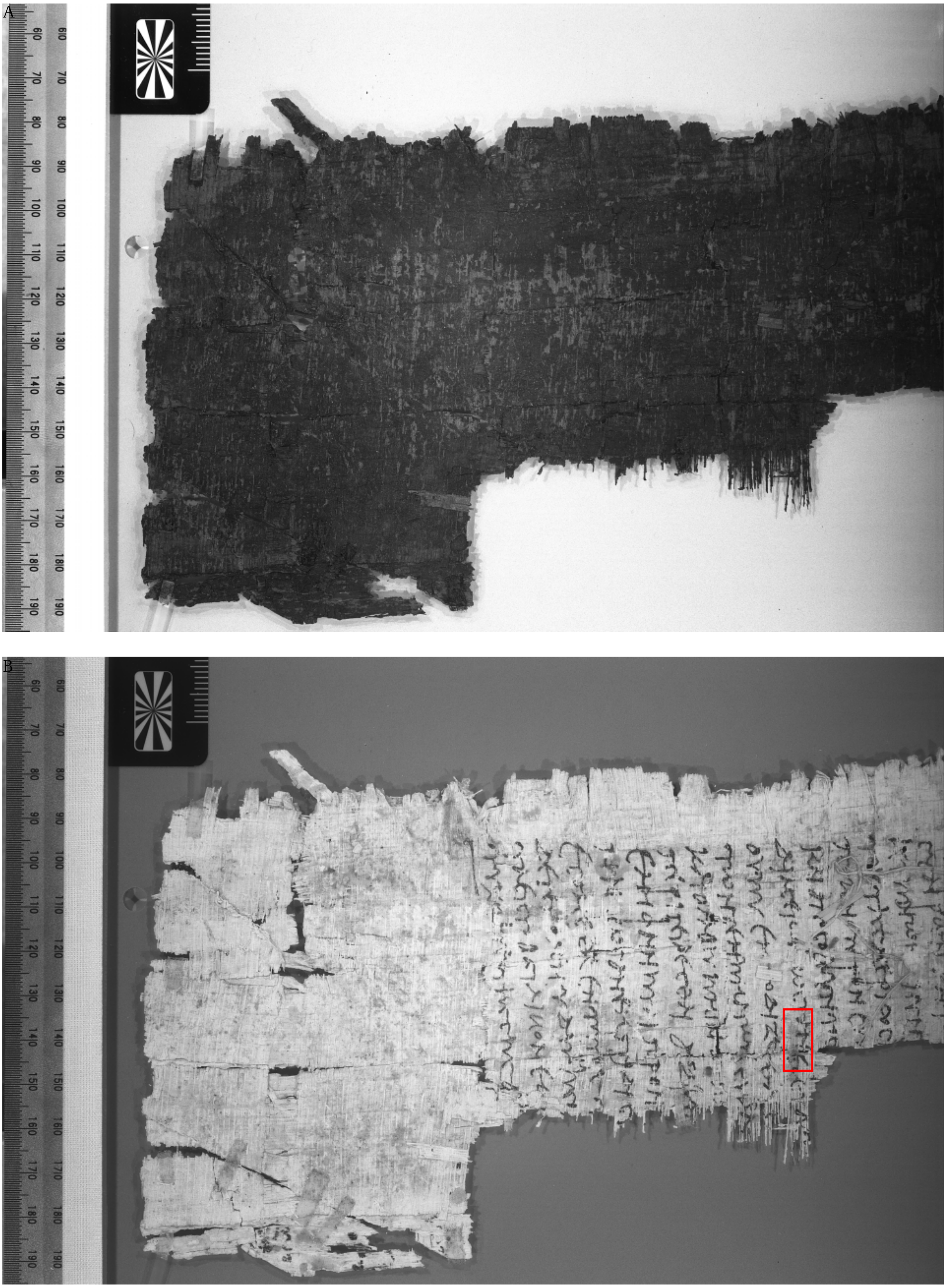

Figure 5. Images at two different wavelengths taken of Tebtunis papyrus 254 at the Bancroft Library, University of California, Berkeley (see http://dpg.lib.berkeley.edu/webdb/apis/apis2?invno=0254&sort=Author_Title&item=1; the reader can see high resolution color images at that link as well). Figure 5A is an image at 450 nm, in which the text is not legible or even visible in most places. The image at 970 nm, 5B, shows the text very clearly. The red box in figure 5B also shows where we picked pixels to create spectra in figure 6.

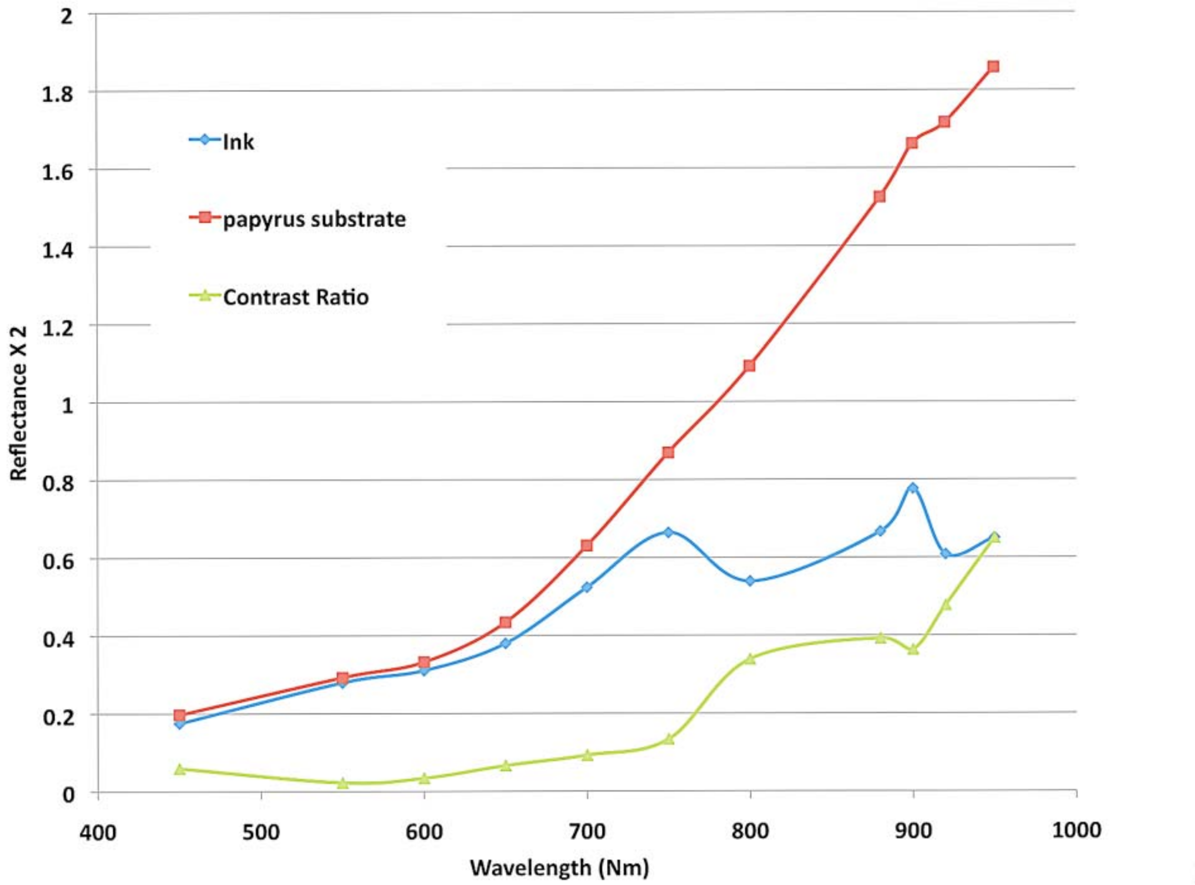

Figure 6. Reflectance spectra of papyrus 254 from Tebtunis Collection. In this case, the ink and papyrus have almost identical reflectance throughout most of the visible, severely reducing the text legibility, as can be seen also in figure 5.

range of the grayscale cardboard background. With some processing the text of the 650 nm images is faint but it is there. By the time we reach 750 nm, the reflectance values are different enough to provide contrast, and the text is quite visible and mostly readable in this area of the fragment; it appears from this data and others that the text is not visible until a ratio of ˜0.25 of ink/substrate reflectance. The Michelson contrast ratio (Michelson, 1927; see http://en.wikipedia.org/wiki/Michelson_contrast-Formulas), a measure of visual contrast, also is plotted in figures 2 and 6. For these figures, the text is easily visible when the contrast ratio reaches ˜0.2.

Note that a monochrome CCD camera is cut off around 700 nm with a short pass filter that blocks out the huge component of solar IR that would swamp a visible black and white image; it would also not see any contrast. In all of these cases, the scholar is faced with seeing a 'black cat at midnight': the absence of contrast between the ink and parchment leaves the text illegible. IR imaging is successful because the parchment reflectance increases in the IR while the ink is relatively flat, thereby increasing the contrast significantly. It is still unknown why this happens for these fragments, but it is not necessary to know why in order to capitalize on this feature.

By analogy with IR imaging of texts, IR has been used over the years with ostraca, again with varying degrees of success and understanding (Cross, 1962; Rosenbaum & Seger, 1986). The Khirbet Qeiyafa ostracon was imaged extensively over the visible and near infrared (400–1000 nm) using a variety of techniques in both Jerusalem and the United States. In addition to providing images to improve readings of the text, we took advantage of this opportunity to investigate the hows and whys of IR imaging of ostraca. In addition, we imaged ostraca from the Tebtunis collection in July 2009 as additional case studies. Based on what we learned, we can say that previous successful IR imagers of ostraca were lucky!

Spectral imaging acquires a complete spectrum for each pixel in the image, which can

Figure 7. Two additional images of Tebtunis papyrus 254; 7a at 650 nm and 7b at 750 nm.

then be used to classify the image into various components (for a brief description and links to more complete references, see http://en.wikipedia.org/wiki/Hyperspectral_imaging). An example of this process is seen in forestry images; even though trees look green from the air, an image cube can be used to distinguish tree species over large areas, based on slight differences in their spectra. There are powerful software tools and algorithms available from other disciplines, such as remote sensing and biology, which can be used to analyze image cube data.

While spectral imaging was required to determine the mechanism of IR imaging, one of the major benefits of the Dead Sea Scroll work and that of papyri imaged by a group at Brigham Young University was the discovery that there is no need to collect all the spectral data, especially for day-in, day-out imaging (Chabries *et al.*, 2003). For the Dead Sea Scrolls, we determined that a single image at ~940–970 nm provides maximum contrast; this is a consequence of the fact that the spectra of the ink and writing substrate are relatively featureless, without sharp peaks and dips. The ink used in the Dead Sea Scrolls (Nir-el & Broshi, 1996; Ginnell, 1993), and most documents prior to c. the 3rd Century CE (most likely of the Khirbet Qeiyafa ostracon as well) was of carbon black in a binder, which is typically flat spectrally. We show below that the ostracon spectra are also relatively featureless, without sharp peaks. Unless many spectral features are present (*e.g.*, color in paintings, frescoes, illuminated manuscripts), the power of spectral imaging is that it can guide one to an effective single wavelength that enables less complex and expensive production imaging. As shown below, spectroscopy produced similar results for the Khirbet Qeiyafa ostracon.

The Khirbet Qeiyafa Ostracon

Imaging

In November 2008, we imaged the Khirbet Qeiyafa ostracon at four laboratories with different equipment and techniques. These were:

1. Headwall Photonics, Fitchburg, MA

Headwall (http://www.headwallphotonics.com) makes and sells pushbroom imaging spectrometers. We were able to image the ostracon in two spectral ranges, 400–800 nm and 800–1100 nm. The spectral resolution was quite high, ~4 nm and the image size was ~1400x800 pixels. The pushbroom method required moving the ostracon past the instrument with a linear translation stage.

2. CRI Inc., Woburn, MA

CRI sells imaging spectrometers that use a proprietary spectral tuning method (http://www.cri-inc.com). We imaged from 450–950 nm with a nominal bandwidth of 20 nm and an image size of 1400 x 1000 pixels. In addition, we did fluorescence imaging, exciting with several blue, green and red wavelengths.

3. MegaVision, Inc., Santa Barbara, CA

MegaVision, a vendor of high-end digital camera backs based on CCD arrays with very large pixel counts, has teamed with Bill Christens-Barry of Equipoise Imaging to use LED illumination panels for spectral imaging. In this method, the spectral component is provided by fixed wavelength light emitting diodes (LED), thus any monochrome camera can be used for imaging. A significant advantage is the ability to obtain much larger images and increased spatial resolution over the other methods, using a medium format camera with a digital back. We used a 39 MP back and 12 narrow spectral bands (~25 nm WHM) centered at the following wavelengths: 355, 450, 465, 505, 535, 592, 625, 638, 730, 780, 850 and 940 nm.

4. Cedars-Sinai Medical Center Imaging Laboratory

Cedars-Sinai has a biomedical imaging laboratory devoted to the development of new technologies. We utilized several of these, in particular, FLIM (fluorescence lifetime imaging) and polarization imaging.

The Results

Figure 8 shows the spectra of the ink, the pottery substrate and of some of the voids in the surface. The surface voids are most likely where larger particulates in the clay fell out of the finished pottery. Since these trap light, they look dark and can be mistaken for ink or text. Figure 9 shows the locations of the three spectral regions of interest (ROI) on the ostracon. As with the scrolls and papyri, the spectra are relatively broad and suggest that the red part of the spectrum is more significant. The maximum re-

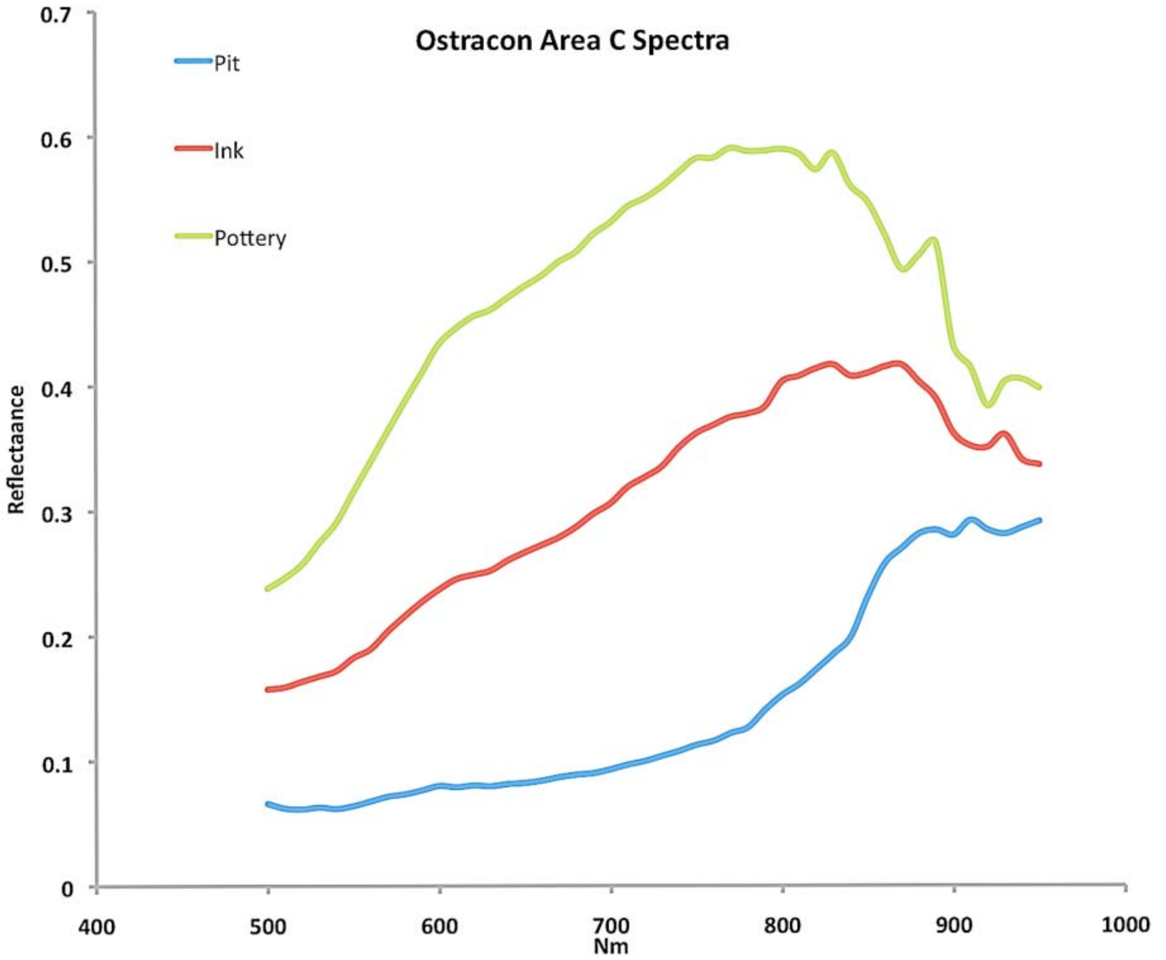

Figure 8. Measured reflectance spectra of the Khirbet Qeiyafa ostracon showing data for the ink, pottery substrate and voids. The spectra are taken from a cube from the CRI data; the cube was flat-fielded to correct for illumination gradients and normalized to unit exposure time.

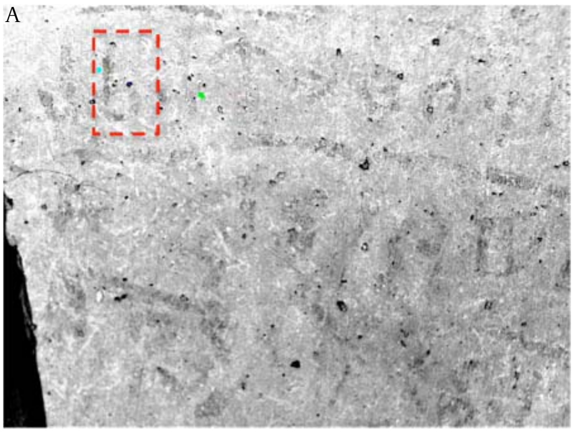

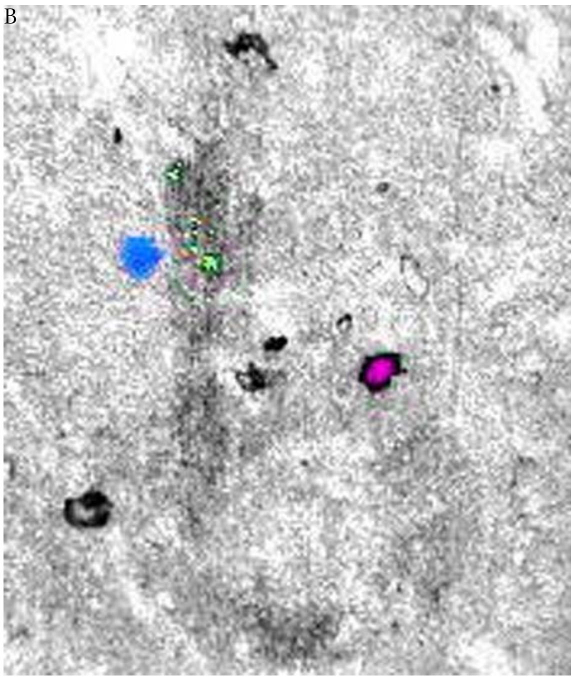

Figure 9. Locations of the pixels used to calculate the spectra of figure 8. A) is a large scale image of the ostracon, showing the upper left and an inset box. B) shows the inset in detail, with the pixels color coded for ink, pottery and voids. Those pixels with hand selected with a software pointing tool.

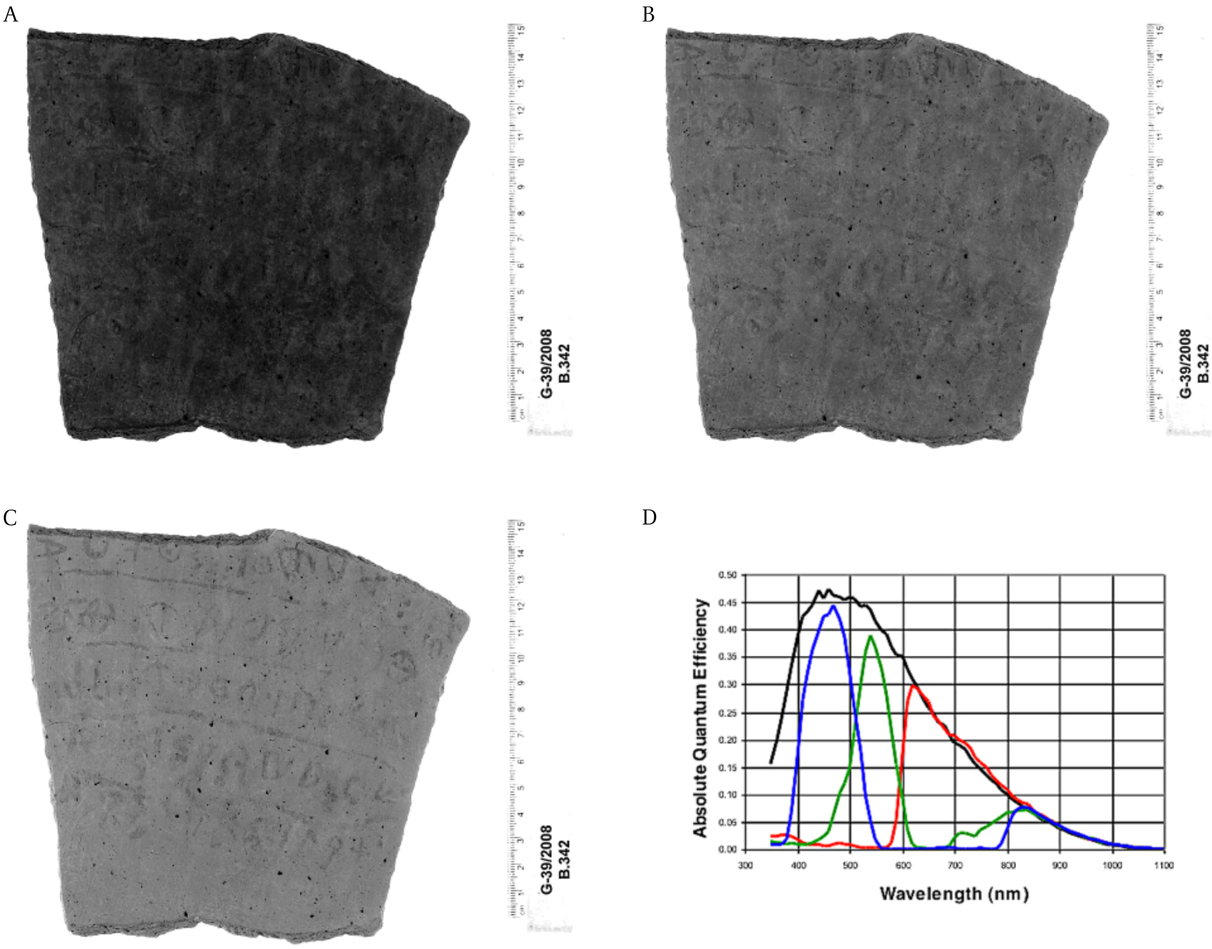

Figure 10. Decomposed color image of Khirbet Qeiyafa ostracon. A) Blue channel; B) Green channel; C) Red channel; D) Inset 10d shows the spectral response of a typical color camera; note the extended response of the red channel. In a color camera, the IR past ˜ 700 nm is blocked with a filter, although the camera response continues out to 1000 nm.

flectance of the pottery is at about 800 nm, but the maximum difference between the ink and pottery background reflectance is at ˜780 nm, although it is rather flat at the maximum.

As with the Dead Sea Scrolls, we determined that imaging the ostracon at a single wavelength could provide the high contrast needed for reading the text. We did apply a variety of sophisticated image segmentation algorithms to the image cube, in particular principal components analysis and spectral classification using user-defined spectral libraries of the pottery, ink and voids. For his work, the epigrapher used primarily single wavelength images (780 nm) that were heavily processed and false colorized, as well as results of the principal components analysis with post processing.

The importance of the red and infrared is clearly evident when decomposing a color image of the Khirbet Qeiyafa ostracon into red, green and blue components, as in figure 10.

Figure 11. Red channel only from the color image of ostracon in figure 12. The red channel was separated from the color image and the processed by setting the black to the ink and white to the pottery (eliminated white background) and then equalized.

Figure 12. Original color image of the ostracon provided by the IAA, with no processing of any sort.

The blue channel is faint and with low contrast, the green shows more of the text, the red still more. Adjusting the histogram and other image processing does not help with the blue image; there is no data there. Figure 11 shows the red channel with equalized histogram; it compares reasonably well with the 780 nm images. Figure 12 is a color image taken by the IAA (as is from the photographer). Actually, one can do this with published images online of ostraca and get pretty reasonable results relative to the color image; that is, *one may be able to obtain improved readings without having to re-image the ostraca*; the authors have extensive experience with field imaging trips and heartily

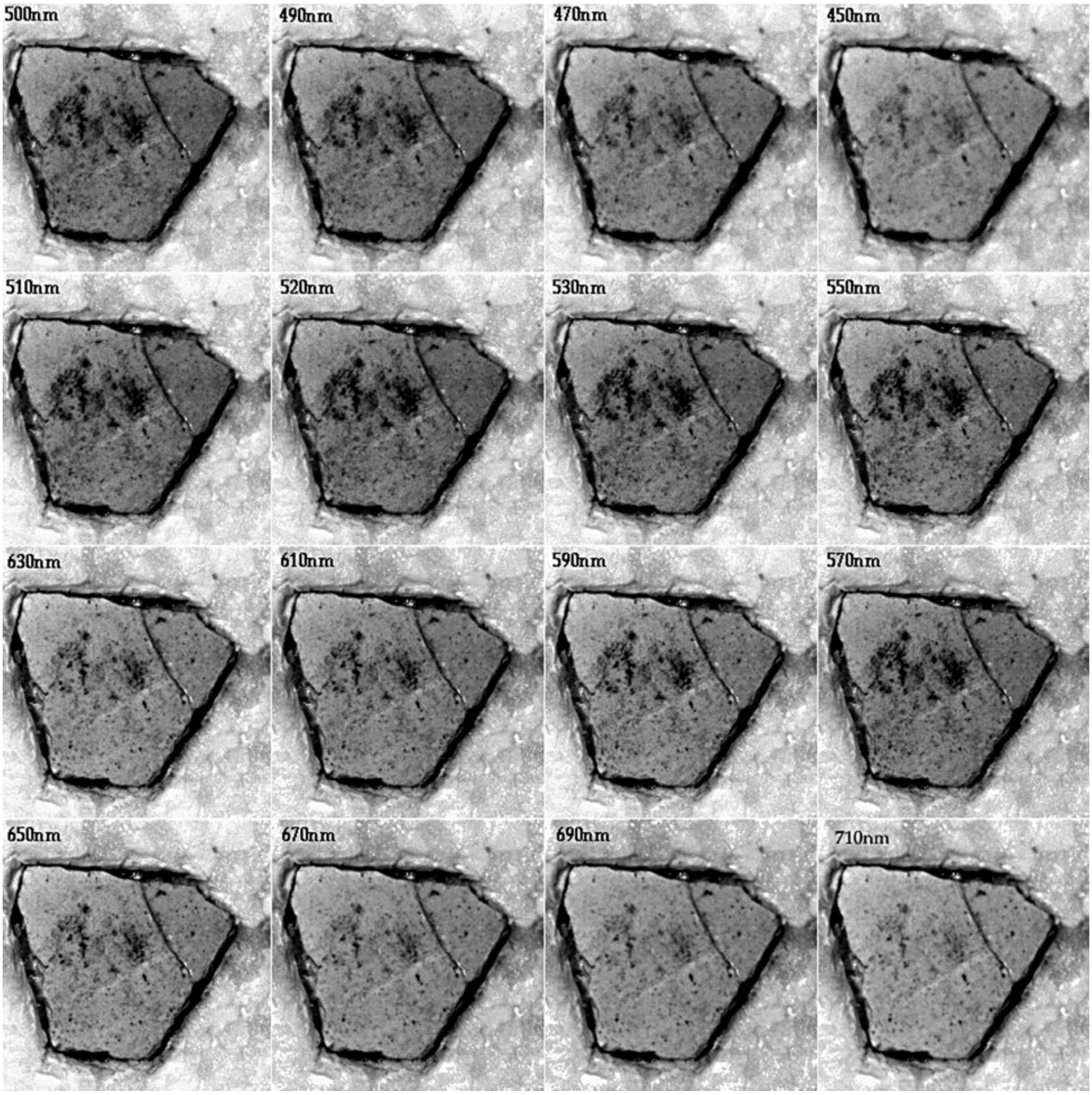

Figure 13. A collage of images of an ostracon with red ink excavated by Zeev Meshal at Kuntillet Ajrud. These images were acquired in July, 1994, shortly before the object was returned to Egypt as part of the Sinai accords.

endorse this approach. In this mode, the color image provides, in the red channel, an image out to ˜720 nm. The spectral transmission of the color Bayer filters on a typical color camera are shown in figure 10D; the red channel actually never turns off and goes out to about 1000 nm, but is blocked for color imaging with a filter. Removal of the filter and replacement with a longpass filter can turn a digital SLR into an IR imager in any channel, although the red has a much larger signal. This is exactly what Bearman did years ago for the Dead Sea Scrolls. The IAA has had a dedicated IR imager since 1997, using a PC-operated tethered monochrome camera with a 940 nm bandpass filter. Bearman replaced it with a similarly modified color Canon SLR during the summer of 2008. Another recent publication has also emphasized the utility of off-the-shelf cameras (Verhoven, 2008).

The importance of the red component of an ostracon color image was independently recognized by Adam Bulow-Jacobsen (2008). Our current work, done at almost the same time, confirms his observation, provides an explanation, and points out some directions to improve imaging. As Bulow-Jacobsen also points out, by decomposing the RGB channels and working only with the red, one can use previous color images of ostraca. For many ostraca, this is an understandable finding: typically in black inks (carbon of some sort) on reddish pottery, ostraca are ideal for infrared imaging. The reflectance of the pottery increases significantly above ˜ 600 nanometers, which is why it appears red, and generally continues to increase up to 1000 nanometers, where silicon CCD cameras and spectrometers become insensitive. So, in general, the reflectance of the pottery background is increasing in the red as a result of the ostraca material. If, however, the ink were some other material, such as ochre, a reddish mineral pigment, or if the substrate were stone, plaster, or pottery with a colored slip, the text and substrate would not increase in contrast in the longer wavelengths and without spectral imaging, the results would be poor for some unknown reasons. Figure 13 shows a collage of images from a spectral cube of an ostracon from Kuntillet Ajrud in the Sinai, dating from the 8th Century BCE; in that case, the contrast was actually maximum in the green (˜540 nanometers) and the text actually disappeared at ˜720 nanometers and longer.

The data of figures 5 and 6 were taken in July 2009, when one of the authors (Bearman, working with the Ancient Text Imaging Group at Brigham Young University) acquired spectral image cubes of both ostraca and papyri from the Neptunis Collection at the University of California in Berkeley. We see the same behavior for the ostracon as for the one from Khirbet Qeiyafa: spectra of a legible text show that the ink and pottery have different reflectance spectra, as in figures 14 and 15. Spectra of illegible, faint or vague text demonstrate, as in figures 16 and 17, that reflectance of the ink and pottery is much closer.

One problem for which we can use the full power of spectral imaging is differentiating between remnants of text and voids and pits in the pottery (the same applies to texts with holes in them, unless backlit). As shown in figure 8, the spectra of pits and voids are very different from those of pottery and ink. Figure 18 shows the results of a minimum noise transformation (a version of a principal components analysis) of an ostracon cube. The larger pits are visible in the color image but some areas of confusion remain. There are three major spectral image components, according to the eigenvalues, all three used to create a composite RGB image. The pits show up clearly as very dark blue. Figure 19 shows another approach to locating the pits: we used a fluorescence spectrum to classify the image. The pits show up as white, along with a shadow of the text. Or, one could build a mask of the pits and apply it to the entire image. Actually, it turns out that the voids are different from the rest of the object and can be segmented in a variety of ways.

As a final summary of images, figure 20-22 show some of the other images used by the epigrapher as part of the transciption and reading of this ostracon.

Other Imaging Techniques

One may naturally ask if there are any other imaging techniques, spectral or otherwise, that would be useful for ostraca. There are a few things that may be worthwhile, based on this work:

1. Polarization imaging. Many ostraca have shiny spots on them that show up very bright in images due to specular reflection. These spots may not only cover text but are visually dis-

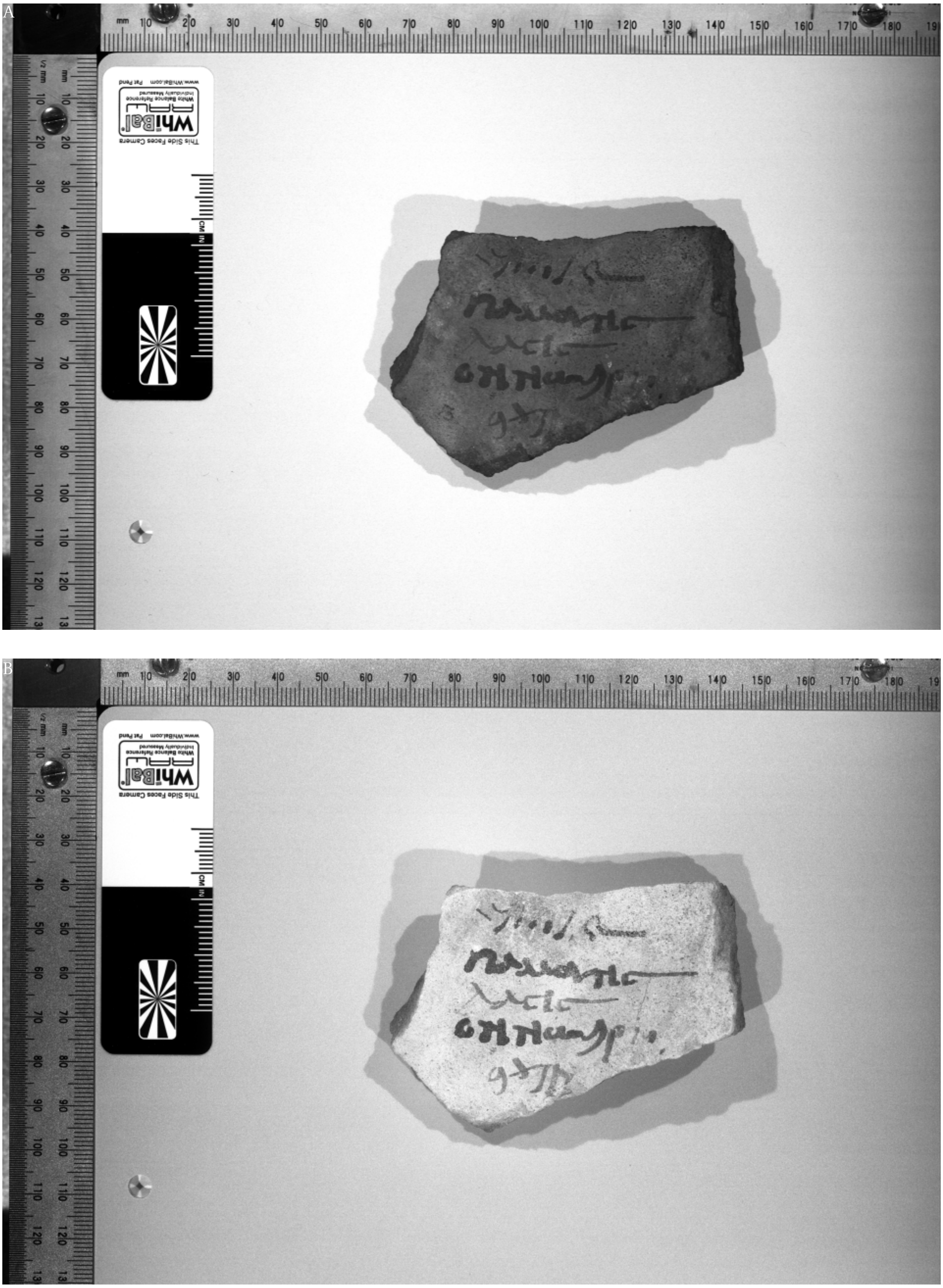

Figure 14. Images of Tebtunis ostracon O.Tebt.20 at 450 nm and 970 nm. For a a high resolution color image see http://dpg.lib.berkeley.edu/webdb/apis/apis2?invno=&genre=Ostraka&institute=Bancroft+Library%2c+Univ.+of+Calif.%2c+Berkeley&sort=Author_Title&item=19

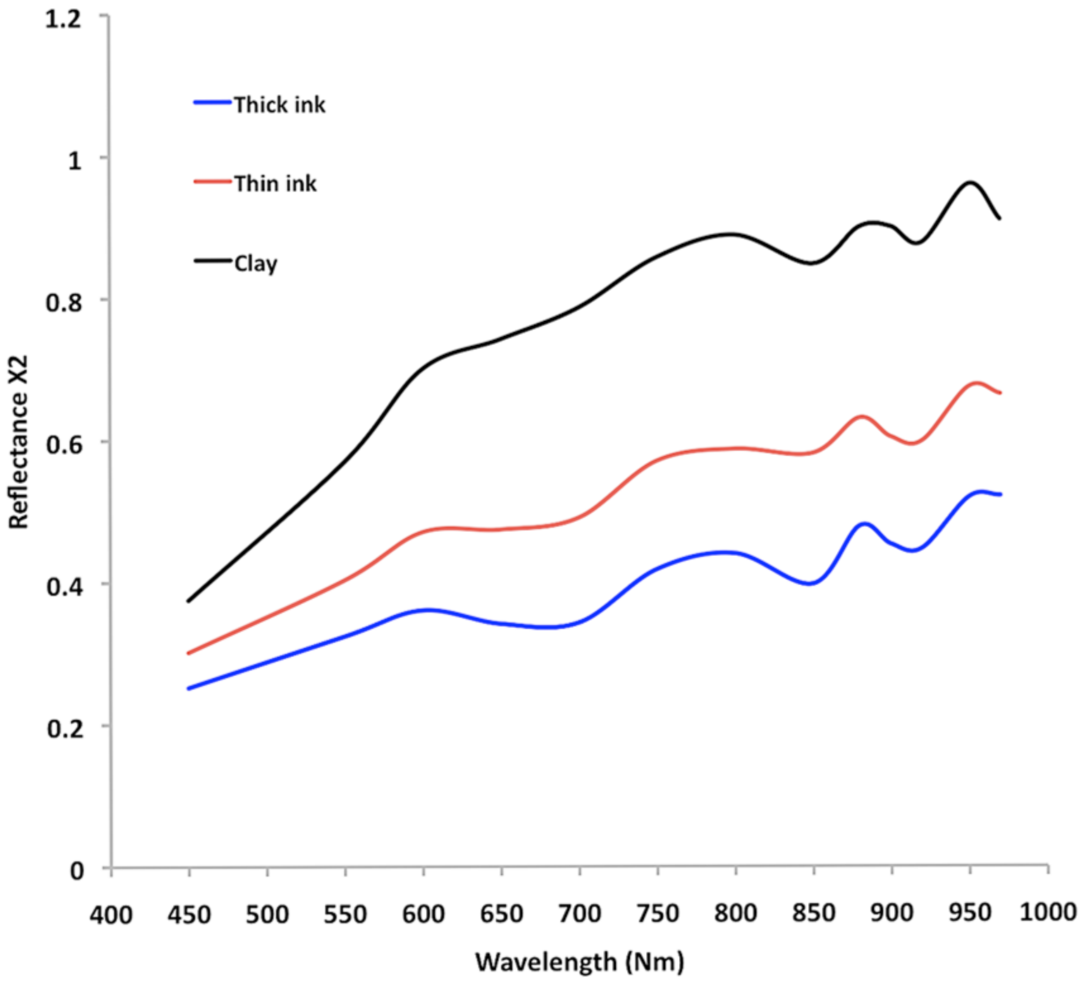

Figure 15. Spectra of the text and clay of figure 14.

tracting to our neural net processor used to read them. In addition, they can saturate and either bloom over to other pixels or make any quantitative analysis of those pixels impossible. These spots typically are encrusted salts and deposits from being exposed to the water table and rain before excavation. Specular reflection typically can be removed by polarization imaging, namely polarizing the illumination and then looking through an analysis polarizer oriented 90 degrees to the illumination one.

2. A second useful method may be one of the several computational imaging methods that can provide the ability to digital manipulate the illumination. Since this ostracon has a fair amount of curvature, it is hard to obtain diffuse, normal or raking lighting for large portions simultaneously. Even doing it in sections means that it cannot easily be stitched together. A combination of something like polynomial texture mapping and spectral imaging would, perhaps, be the ultimate imaging of this object. We also applied other image processing techniques to the ostracon spectral image cubes as well as to the ostracon images.

This ostracon had significant striations on the surface that were visually distracting and interfered with the visibility of the text. These striations, which all ran in one direction, were created when the pot was turned on a potter's wheel. Fourier techniques can be used to perform filtering operations to reduce undesirable image features having periodic or regular structure; this type of operation is referred to as 'spatial filtering'. The Fast Fourier Transform (FFT) is a computationally efficient algorithm for computing the forward and inverse Fourier transforms of an image used in spatial filtering. Filtering the power spectrum correctly can remove the high frequency striations and leave

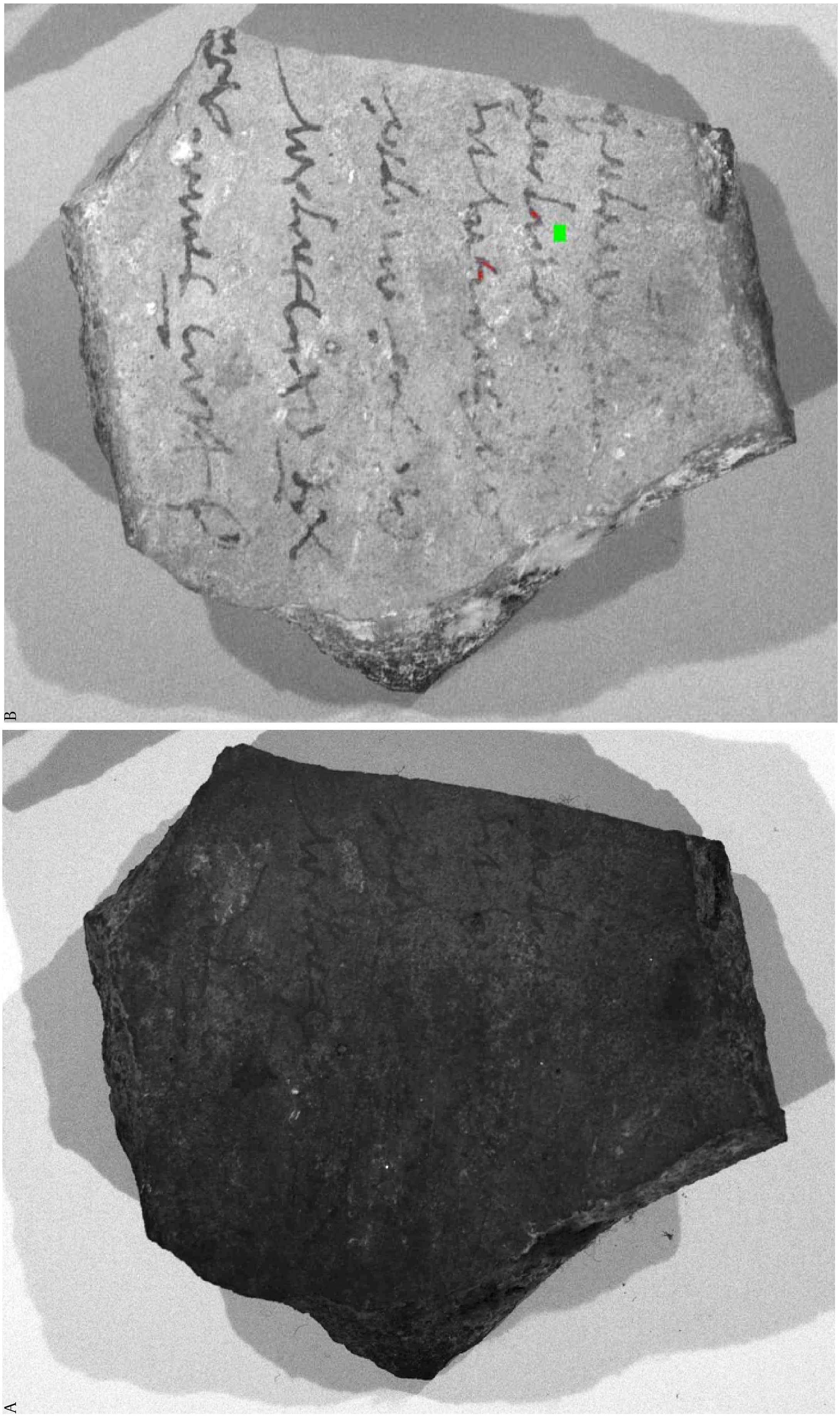

Figure 16. Two images of O.Tebt.06 from the Tebtunis collectin at Bancrafto library. See http://dpg.lib.berkeley.edu/webdb/apis/apis2?invno=&genre=Ostraka&institute=Bancroft+Library,+Univ.+of+Calif.,+Berkeley&sort=Author_Title&item=24 for details and high resolution color images. The colored pixels in B) show the pixels used to create the spectra of figure 17.

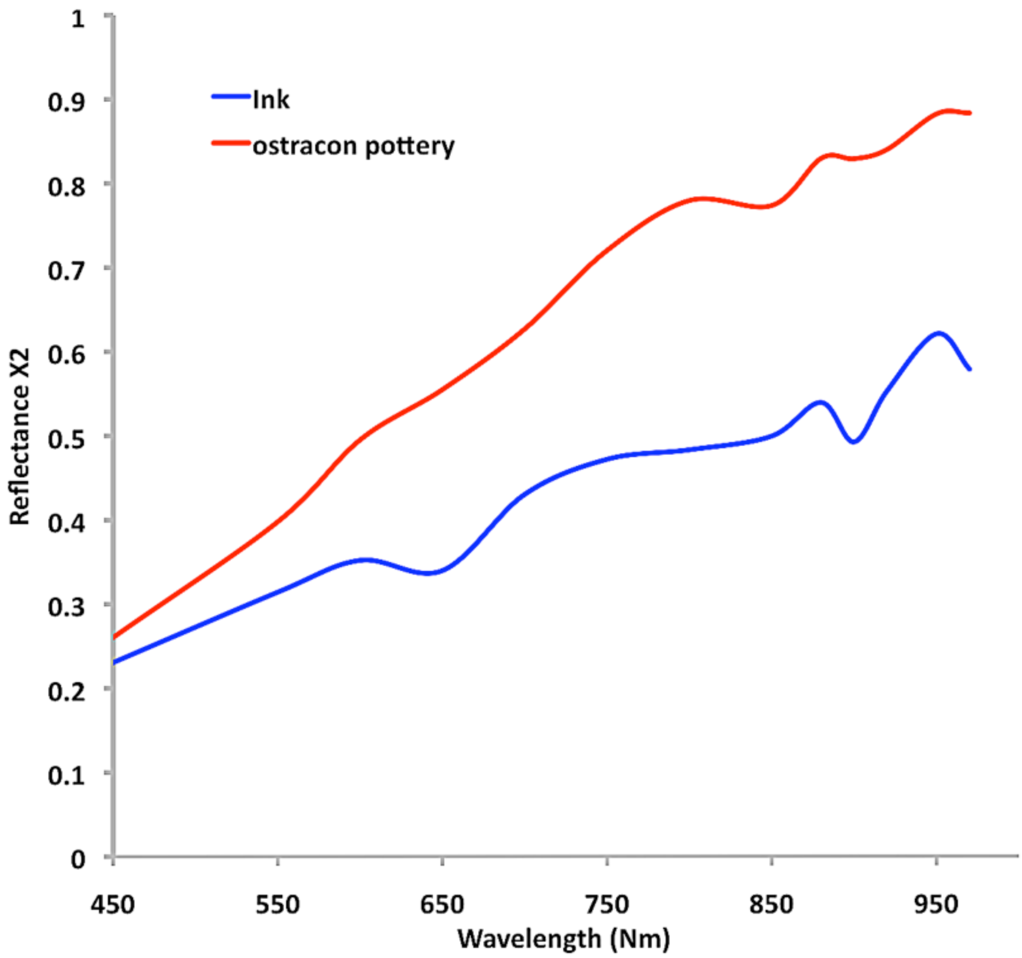

Figure 17. Reflectance spectra of the ostracon in figure 16.

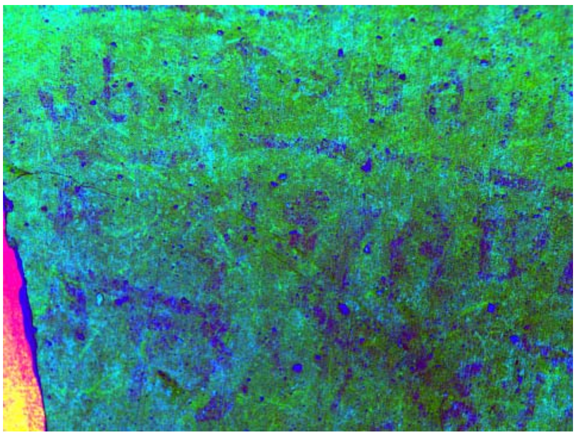

Figure 18. Minimum noise transformation of a flattened cube. There are three significant eigenvalues, corresponding to the ink, pottery background and the pits. This is an RGB of the three eigenimages, mapped in RGB. The pits show up as a very vivid dark blue and there are many areas where they overlap with text and not visible in the color images taken by the Israel Antiquities Authority.

the text and background intact. Before and after images showed significant reduction in the striations; careful application of the filter can remove unwanted image artifacts with minimal alteration of desired image features. Our conclusion is that FFT filtering can take out periodic features but that it should be done with filters tuned specifically for the image, noise and artifact to be removed or reduced.

We also used Markov texture feature analysis to examine local pixel correlation to reveal features not apparent with first order statistics such as mean, variance and other manipulations of the pixel values via histogram functions. To date, the Markov analysis shows local pixel correlation that we identify with the striations on the ostracon surface, and can distinguish surface pitting from dark patches of similar shape and size.

Some local operators can also do a reasonable job of locating pits in the surface. Figure 20 shows an image of the Khirbet Qeiyafa ostra-

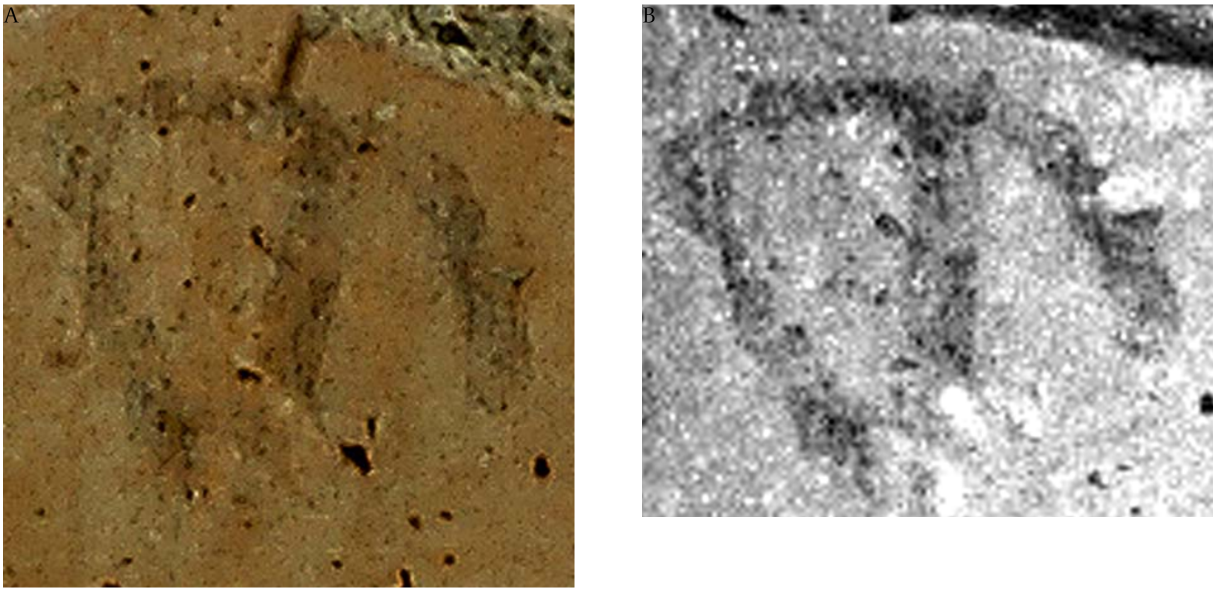

Figure 19. Minimum noises transformation of the fluorescence spectral cube that differentiates ink, pottery and surface voids. In this case, one of the voids lies directly on the text. A) is zoomed in on a character from 5B, while B) shows one of the MNF image planes, with the pits showing as very bright.

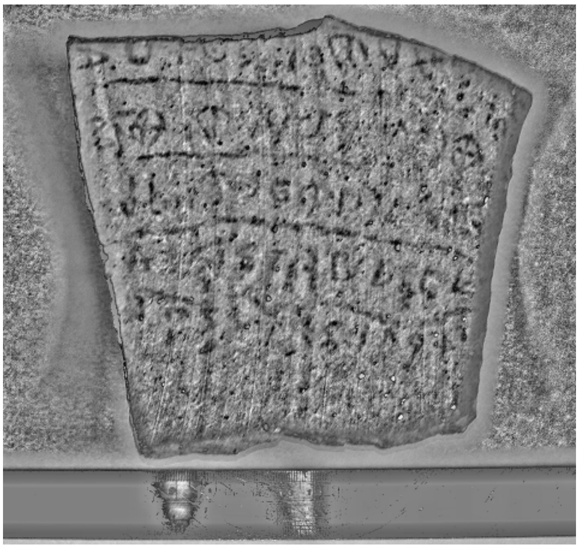

Figure 21 (above). One of the processed images used by the epigrapher.

Figure 20 (left). A heavily processed image with a moving local operator.

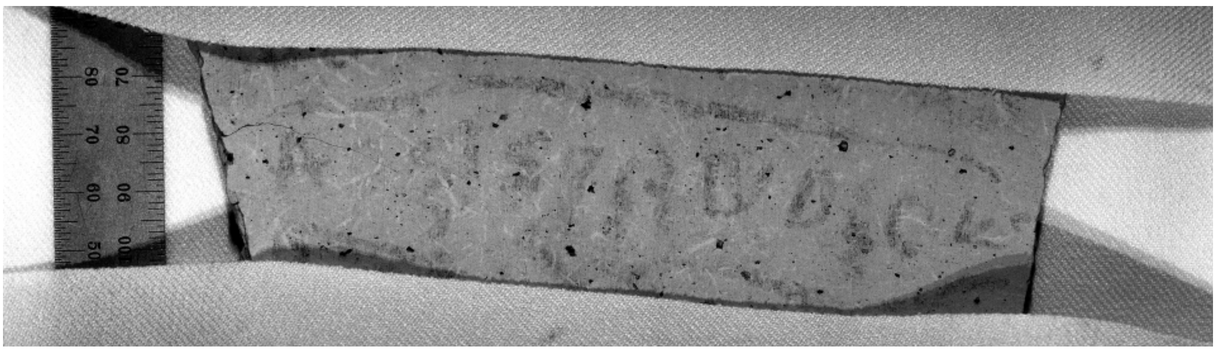

Figure 22. A high-resolution image of a line of text taken with a39 MP camera at Mega-vision. We did it in sections in an attempt to compensate for the curvature. The image has been flattened with an *a posteriori* algorithm (http://helios.univ-reims.fr/Labos/INSERM514/ImageJ/#shading_correction) since we had turned to camera for some of the imaging and could not reconstruct the white image we had previously acquired.

con in the IR; it was processed with a 100 pixel square neighborhood operator which equalized the local mean and variance at every pixel in the image. In this case, the pits also show up quite easily.

Acknowledgements

The images from Tebtunis are courtesy of the Bancroft Library, University of California, Berkeley. The data taken there was acquired with equipment and the help of the Ancient Text Imaging Group at Brigham Young University, directed by Roger McFarlane. The Kuntillet Ajurd images are courtesy of Zeev Meshal and the Dead Sea Scroll images are available courtesy of the Israel Antiquities Authority and Pnina Shor. A very special thanks to Saar Ganor who hand carried the ostracon from Israel and around the United States for imaging.

Cited Literature

Attas, M., E. Cloutis, C. Collins, C.M. Goltz, C. Majzels, J. Mansfield & H. Mantsch. 2003. Near-Infrared Spectroscopic Imaging in Art Conservation: Investigation of Drawing Constituents. – Journal of Cultural Heritage 4: 127–136.

Baronti, S., A. Casini, F. Lotti & S. Porciniai. 1997. Principal Component Analysis of Visible and near-Infrared Multispectral Images of Works of Art. – Chemometrics and Intelligent Laboratory Systems 39: 103–114.

Beardsley, N.F. 1936. The Photography of Altered and Faded Manuscripts. – The Library Journal 61: 96–99.

Bearman, G.H. & S. Spiro. 1996. Archeological Applications of Advanced Imaging Techniques. – Biblical Archaeologist 59: 56–66.

Bearman, G.H., S. Pfann & S. Spiro. 1998. Imaging the Scrolls: Photographic and Direct Digital Acquisition. In: Flint P.W. & J.C. Vanderkam. Eds. 1998. The Dead Sea Scrolls after Fifty Years: A Comprehensive Assessment. Volume I. – Leiden, Brill: 472–495.

Bearman, G.H., B. Zukerman, K. Zuckerman, & J. Chiu. 1993. Multi-spectral Imaging of Dead Sea Scrolls and other Ancient Documents. Paper presented at the 1993 Annual Meeting of the American Academy of Religion and Society of Biblical Literature. – Washington D.C., Society of Biblical Literature.

Bulow-Jacobsen, A. 2008. Infra-Red Imaging of Ostraca and Papryi. – Zeitschrift für Papyrologie und Epigraphik 165:175–185.

Chabries, D.M, S.W. Booras & G.H. Bearman. 2003. Imaging the Past. – Antiquities 77: 359–372.

Cross, F.M. 1962. Epigraphic Notes on Hebrew Documents of the Eighth-Sixth Centuries B.C. II. The Murabba'at Papyrus and the Letter Found near Yabneh-Yam. – Bulletin of the American Schools of Oriental Research 165: 34–46.

Delaney, J.K., E. Walmsley, B.H. Berrie & C.F. Fletcher. 2005. Multispectral Imaging of Paintings in the Infrared to Detect and Map Blue Pigments. In: [Edited by National Academy of Sciences]. Scientific Examination of Art: Modern Techniques in Conservation and Analysis (Sackler NAS Colloquium). – Washington D.C., Proceedings of the National Academy of Sciences: 120–136.

Edwards, H.G.M., D.W. Farwell, F.R. Perez & S.J. Villar. 1999. Raman Microscopy of a Mediaeval Spanish Cantoral. – Applied Spectroscopy 53: 1436–1439.

Edwards, H.G.M. & F.R. Perez. 2004. Application of Fourier Transform Raman Spectroscopy to the Characterization of Parchment and Vellum. II. Effect of Biodeterioration and Chemical Deterioration on Spectral Interpretation. – Journal of Raman Spectroscopy 35: 754–760.

Ferrer, N. & M.C. Sistach. 2005. Characterisation by Ftir Spectroscopy of Ink Components in Ancient Manuscripts. – Restaurator: International Journal for the Preservation of Library and Archival Material 26: 105-117.

Ginnell, W. 1993. Report on Dead Sea Scroll Studies. – Getty Conservation Institute Report.

Goltz, D.M., E. Cloutis, L. Norman & M. Attas. 2007. Enhancement of Faint Text Using Visible (420–720 Nm) Multispectral Imaging. – Restaurator: International Journal for the Preservation of Library and Archival Material 28: 11–28.

Havermans, J., H.A. Aziz & H. Scholten. 2003a. Non Destructive Detection of Iron Gall Inks by Means of Multispectral Imaging Part 1: Development of the Detection System. Restaurator: International Journal for the Preservation of Library and Archival Material 24: 55–60.

Havermans, J., H.A. Aziz & H. Scholten. 2003b. Non Destructive Detection of Iron-Gall Inks by Means of Multispectral Imaging. Part 2: Application on Original Objects Affected with Iron-Gall-Ink Corrosion. – Restaurator: International Journal for the Preservation of Library and Archival Material 24: 88–94.

Lee, A.S., P.J. Mahon & D.C. Creagh. 2006. Raman Analysis of Iron Gall Inks on Parchment. – Vibrational Spectroscopy 41: 170–175.

Mannucci, E., R. Pastorelli, G. Zerbi, C.E. Bottani & A. Facchini. 2000. Recovery of Ancient Parchment: Characterization by Vibrational Spectroscopy. – Journal of Raman Spectroscopy 31: 1089–1097.

Mansfield, J.R., M.G. Sowa, C. Majzels, C. Collins, E. Cloutis & H.H. Mantsch. 1999. Near Infrared Spectroscopic Reflectance Imaging: Supervised vs. Unsupervised Analysis Using an Art Conservation Application. – Vibrational Spectroscopy 19:33–45.

Marengo, E., E. Robotti, M.C. Liparota & M.C. Gennaro. 2003. A Method for Monitoring the Surface Conservation of Wooden Objects by Raman Spectroscopy and Multivariate Control Charts. – Analytical Chemistry 75: 5567–5574.

Michelson, A. 1927. Studies in Optics. – Chicago, University of Chicago Press.

Nir-el, Y. & M. Broshi. 1996. The Black Ink of the Qumran Scrolls. – Dead Sea Discoveries 3: 157–167.

Plenderleith, H.J. 1950. Comment on a Paper Entitled: Recent Discoveries in Biblical Manuscripts. – Journal of Transactions of the Victoria Institute: 82.

Rosenbaum, J. & J.D. Seger. 1986. Three Unpublished Ostraca from Gezer. – Bulletin of the American Schools of Oriental Research 264: 51–60.

Ross, K. 1933. Zur Photographie mit ultraviolettem und infrarotem Licht. – Zeiss Nachrichten 4: 19–27.

Tanner, S. & G.H. Bearman. 2009. Digitizing the Dead Sea Scrolls. Imaging Science and Technology. – Washington, www.imaging.org (IS&T conference proceedings).

Verhoeven, G. 2008. Imaging the Invisible Using Modified Digital Still Cameras for Straightforward and Low-Cost Archaeological Near-Infrared Photography. – Journal of Archaeological Science 35: 3087–3100.

Submitted: 10 November 2009
Published: 1 December 2009
Revised (first author's email address and acknowledgement): 10 February 2010